International Journal of Applied Engineering
Research and Development (IJAERD)
ISSN(P) 2250-1584; ISSN(E): 2278-9383
Vol. 3, Issue 5, Dec 2013, 7-14

STUDY OF THE DEVELOPED NANO- SCALE PRECIPITATES IN AF/C 489 ALLOYS BY USING DSC AND SEM TECHNIQUES

E.F. ABO ZEID[1], A. GABER[2], M.A. GAFFER[3], LAMIAAGALAL[4]

[1,2,3,4]Department of Physics, Faculty of Sciences, Assiut University, Assiut 71516, Egypt

[1]Department of Physics, Faculty of Science and Arts, Al Baha University, KSA

ABSTRACT

In the present article, kinetics of the clustering processes in AF/C489 Alloyin the early stages of aging was probably contributed by coalescence of Cu-vacancy, Li-vacancy and Zn-vacancy complexes to form Li–Cu-Zn-vacancy clusters. The high value of the activation energy indicate that the driving force of the clustering process is high.In Li-containing aluminium alloy, preferential clustering of lithium-vacancy pairs is thought to occur during solution treatment and quenching, since lithium possesses a higher vacancy binding energy than zinc or magnesium does.The diffusion of Zn and Mg atoms is slowed down because of preferential formation of Li-vacancy aggregates in the alloy, when Li atoms are present in the form of solution.The activation energy associated with the precipitation of the θ` phase was found 61.63 kJ $mol^{-1}$. Accordingly, the mechanism of the precipitation of θ` (Al_2Cu) phase controlled by both migrations of Li and Cu atoms in the Al matrix.Vacancies bound to lithium atoms make it difficult for diffusion or aggregate to grain boundaries, this is one of the main reasons of forming narrow precipitate-free zones in present Li-containing alloy.The results evidently indicate that Li atoms slow down the diffusion of Zn and Mg atoms and vacancies, and thus the segregation of them to grain boundaries has been restricted.The microhardness was found to increase as a result of the precipitate of δ` (Al_3Li) and T_1(Al_2CuLi) precipitates.

KEYWORDS: AL-Li AF/C 489, microhardness, DSC, δ′-Phase, θ` Precipitates, T_1-Phase

INTRODUCTION

In the last five decades, technological demands for materials having high specific tenacity (strength to weight ratio), high specific modulus, low coefficient of thermal expansion, good wear resistance, low density and good thermal conductivity are constantly increasing. Aluminum offers one answer for the combinations of such attractive properties. The aluminum alloy AF/C 489, which contains copper and lithium, is especially attractive due to its age hardenable properties. These alloys are used for applications involving high temperature exposures up to 300 °C, such as engines for both automotive (engine cylinder heads, pistons etc.) and aircraft applications [1-3]. In order to achieve better fuel efficiency and lower operation cost, aerospace and aviation industries have spent lots of effort looking for new alloy developments of high strength and light weight. Owing to their low density and good mechanical properties, Al–Cu–Li alloys have received extensive attention. Precipitation strengthening is the major strengthening mechanism for Al–Cu–Li [4, 5]. Aluminium alloys containing lithium as a major alloying element rely upon heat-treatment to develop their high- strength potential [6, 7]. Noble and Thompson [8] have summarized the precipitation sequence as a two-stage process: a-supersaturated solid solution →α + δ'($A1_3Li$) → δ (A1Li) Maximum strengthening was found to be associated with precipitation of the metastable ordered Li_2 δ` phase, which grow as coherent spherical particles. Gregson and Flower [9] showed that the strength of A1-Li alloys could be enhanced by additions of magnesium or copper; more recently both these additions have been included in the development of a quaternary AI-Li-Mg-Cu alloy [10]. Furthermore, the presence of such additional

alloying elements might be expected to influence precipitation of δ' itself. Precipitation of δ' phase was accompanied by the formation of additional ternary precipitate phases in the copper containing alloys [11, 12]; however the existence of these phases was found not to influence the nucleation of the δ' which in all cases precedes the formation of the other phases. It was found that, improvement of properties in Al-Li-X alloys requires a clear understanding of precipitation in these systems. Al alloys are commonly considered to make a feature of light weight, high specific strength and high elastic modulus, the effects of high Li-content (more than 1.8 wt%)[13-15] and low Li-content (less than 1.0 wt%)[3] on Al-Zn-Mg-Cu alloys have been investigated widely in recent years. It is evidenced that in higher Li-content alloys (over 1.8 wt% Li), the main strengthening precipitates are δ and/or its transient phases [13-15], while in lower Li-content alloys (under 1.0 wt% Li) they are η' and/or its transient phases [16]. Regretfully, little systematic information was reported on the 1.0 wt% Li-containing Al-Zn-Mg-Cu alloys, especially their phase transformation, microstructure evolution and hardening effects except knowing the absence of the δ phase in it [16, 17-21]. The precipitation sequence and the age hardening behavior of the base alloys change with the lithium content. It is well known that the aging kinetics and precipitation behavior are strongly associated with the interaction between quenched-in vacancies and solution atoms in Li-containing Al–Zn–Mg–(Cu) alloys.[17, 20] suggested that the preferential clustering of Li atoms and vacancies appears to suppress the diffusion of Zn and Mg atoms, and vary the nucleation mode and subsequent precipitation process. The purpose of the present paper is to study the aging behavior of the Li containing Al–Cu–Zn–Mg alloys and to understand and discuss strengthening and microstructure evolution as a function of ageing temperature and time.

EXPERIMENTAL PROCEDURE

The studied Al-Li (AF/C 489) alloy is composed of Al-2.7%wtCu-1.8%wtLi-0.6%wtZn-0.3%wtMg-0.3%wtMn-0.08%wtZr. The **D**ifferential **S**canning **C**alorimetry (DSC) technique was used to follow the precipitation processes which take place in AF/C 489 alloyduring continuous heating at various heating rates ranging from 5-50 K/min of the quenched specimens from the solid solution state. Disc-shaped samples of 5mm diameter and 0.5mm thickness of average weight of ~25 mg were machined from the alloy ingot. The specimens were solution heat treated for 1 h at 803K in a standard convection furnace and then quenched into a mixture of ice and water at equilibrium (~273 K). An annealed pure aluminum disc of similar shape and mass was used as a reference. Non-isothermal scans for the as-quenched specimens using a DSC thermal analyzer (DSC-DO 8T-12TG01 type Shemadzu) were carried out. Scans were performed between room temperature and 773K in purified nitrogen flow at a rate of 30 ml min^{-1}. The output signal was in mW and the net heat flow to the reference material was recorded with temperature. The peak temperature of the reaction processes was identified with an uncertainty of (±0.1 K) using the microprocessor of the thermal analyzer.

For isochronal microhardness (**HV**) measurements, disc shaped specimens of about 15 mm diameter and 2 mm thickness were used. The surfaces of the specimens were mechanically polished. The final polishing was achieved using (Struers) diamond paste of ~0.25 μm grain size and a piece of cloth. Prior to every HV measurement, the specimen surfaces were gently polished by the 0.25 μm diamond paste to remove the surface reactions that may occur during the heat treatment. The microhardness measurements were performed using Vickers method. Each given HV value is the average of at least ten readings distributed over the whole surface of the specimen without paying attention to the positions. The probable error in HV is due to the diagonal of impression measurement, which leads to an overall error in HV of about 3%.

For **S**canning **E**lectron **M**icroscopy (SEM) observations, disc shaped specimens of 10 mm diameter and 1 mm thickness were prepared and polished similar to the microhardness specimens. The specimens were solution heat treated at 803 K for 1 h and then quenched into water maintained at ~273 K. Before microscopic examinations, the surfaces of specimens were gently polished by 0.25 μm diamond paste. Then, the specimens were etched using a solution of

1%HF+2.5%HNO_3 (by volume) in H_2O. The SEM examinations were performed after aging for 20 min at the temperature of the developed precipitate using a scanning electron microscope (SEM, JEOLJSM-5400LV, Japan) at Assiut University.

Transmission **E**lectron **M**icroscopy (TEM) examinations were performed at Assiut University, Egypt. For microstructural examinations, a200kV-TEM (TOPCON- 002B) was used. It was operated at 120 kV to avoid sample damage by the electron beam. Thin foils were prepared from the quenched and aged specimens. Thin discs of 3mm diameter were punched from the foils and then electropolished by the twin-jet technique using a solution of 25% nitric acid and 75% methanol cooled to 243K. The electropolishing was performed using a DC current source operating at ~20V.

RESULTS AND DISCUSSIONS

HV Behavior of the Studied Alloy during Isochronal Annealing

An isochronal annealing regime of previously solution heat treated specimens of AF/C 489 alloy has been suggested to follow the decomposition behavior of the supersaturated alloys as a function of temperature. Normally the specimens were aged for 30 min at temperatures of 20 K intervals starting from room temperature up to 773 K and subsequently quenched into water maintained at ~273K. The microhardness measurements have been performed at room temperature after each quench. Figure 1 shows the variation of HV as a function of the aging temperature.

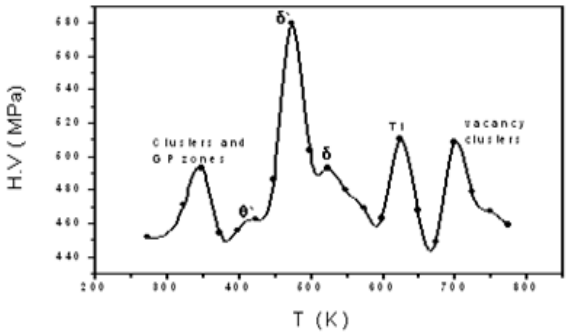

Figure 1: HV vs. Aging Temperature for AF/C 489 Alloy

It is clear that the general behavior of the HV is characterized by six successive reactions labeled as I through VI. The first precipitation peak (I) may be attributed, to the formation of Cu–Li vacancy clusters and GP-zones. This peak appeared at ~345 K. The second precipitation peak (II), which can be attributed to the nucleation of the needle shaped θ` precipitates, which appeared at 415 K. These precipitates are coherent to the Al-lattice and, therefore a strengthening of the alloy would take place. A precipitation of the strengthening spherical δ` precipitates third peak(III) takes place after the completion of the needle shaped θ` precipitates at 475K. The forth hardening precipitates peak (IV), which is measured above 520K for the studied alloy, may be ascribed to the nucleation of plates of $T_1(Al_2CuLi)$ precipitates. After the completion of the T_1 phase, another shoulder increase, peak (V) which can be attributed to the formation of equilibrium plate-like δ ($Al_5Cu_6Mg_2$) phase, which has a limited contribution to the HV (over-aging-case). Above this temperature, a steep decrease in the microhardness was detected up to 690 K. This decrease may be attributed to the dissociation of the precipitated particles. By further increasing temperature the microhardness was found to increase with increasing temperature up to 700K. The abundant concentration of quenched in vacancies in this range of temperatures and the formation of vacancy clusters might explain it. These vacancy clusters have a limited contribution to the microhardness. This result implies that the material should be return to the as quenched state. Since Li atoms possess a high concentration and significant vacancy-binding energy, they preferentially trap the quench-in vacancies, then retard the diffusion of Cu, Zn atoms, and suppress the homogenous nucleation of Cu-rich phases in the matrix [22].

Differential Scanning Calorimetry (DSC)

Figure 2-a: shows typical non-isothermal DSC thermograms of the supersaturated AF/C 489 alloy, performed at different heating rates ranging from 5 to 50 K min^{-1}. The DSC scans were carried out from room temperature up to 800 K. Five exothermic reaction processes can be identified from the DSC thermograms indicated by I through V as shown in Figure (2-b) for representative heating rate of 20 K min^{-1}. It is obvious that the exo-and endothermic reaction peaks are shifted towards higher temperatures as the heating rate increases. This confirms the thermally activated nature of these reactions. First peak I is ascribed to the formation of Cu–Li vacancy clusters and GP zones, where this reaction takes place at a wide range of temperature ranging from 405 to 445 K depending on the heating rate. Peak II, can be caused by the precipitation of the coherent precipitates θ`. The third exothermic peak might be due to θ` transformation to δ` ($Al_3Li$) particles. To confirm this result, an SEM examination was carried out for a specimen heated at a rate of 20 K $min^{-1}$ up to a temperature of 520 K and aged at this temperature for 30 min. Scanning electron microscopy examination revealed δ` (Al_3Li) needle shaped precipitates, as shown in figure (3-a). Peak IV can be explained by the precipitation of the δ ($Al_5Cu_6Mg_2$) phase precipitates. Peak V ascribed to the precipitation of plate like T_1 (Al_2CuLi) phase where this reaction takes place at a wide range of temperature ranging from 610 to 700 K depending on the heating rate. Scanning electron microscopy examination revealed to T_1 (Al_2CuLi) precipitates, as shown in figure (3-b) as a result of aging the specimen for 30 min at 650 K. Small concentration of δphase coexist with T_1 plates this information can be confined by SEM, Figure (3-c).

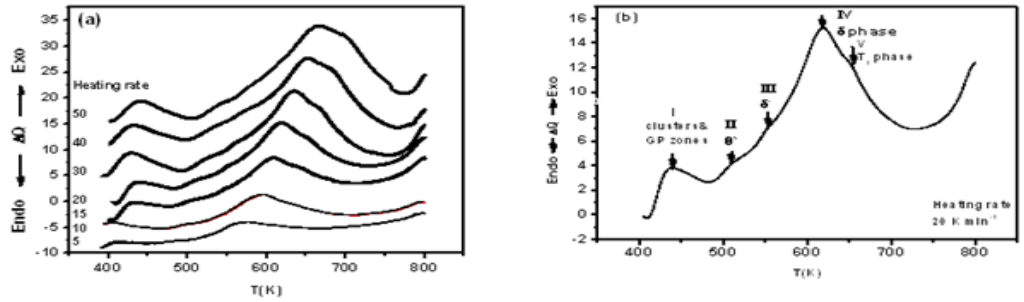

Figure 2: (a) Typical DSC Scans of AF/C 489 Alloy Performed at Various Heating Rates and (b) Representative DSC Scans of AF/C 489 Alloy Performed at Heating Rate of 20 K min^{-1}

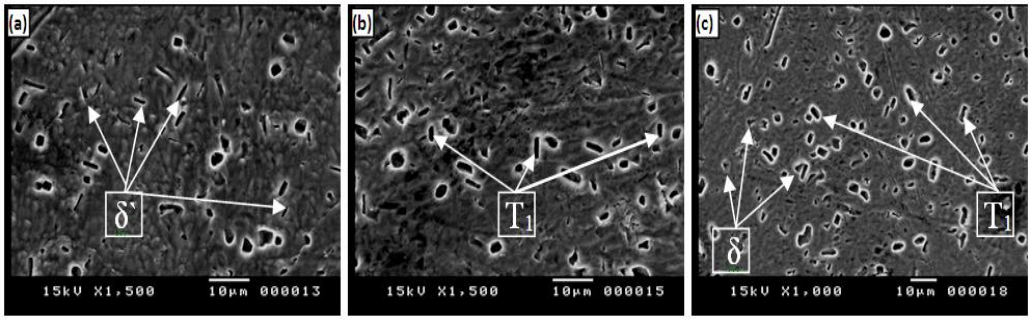

Figure 3: Scanning Electron Micrograph Showing the Typical Distribution of (a) δ` Phase, (b) Plates of T_1-Precipitates and (c) The Coexistence of δ and T_1 as the Specimen Aged at 480°K, 540°K and 650°K for 30 min, Respectively

PHASE TRANSFORMATION MECHANISM

The transformation processes (precipitation and dissolution of the precipitates) are always related to the concept of the activation energy. The study of precipitation processes is also associated with nucleation and growth processes dominating in supersaturated alloys. In general, separate activation energies must be identified with individual nucleation

and growth steps in a specific transformation, although they have usually been combined into an activation energy representative of the overall precipitation process [23]. From the results of the DSC thermograms, the dependence of a certain process peak temperature $T_p$on the heating rate γ can be used to evaluate the activation energy of that process by applying one of the non-isothermal thermo-analytical studies proposed by Kissinger [24] and Starink[25] as shown in table (1). These methods are based on the Avrami treatment of transformation kinetics and define an effective crystallization rate coefficient having Arrhenian temperature dependence. Several different ways of data mathematical treatment have been proposed. Most of them are based on an incorrect neglecting of the temperature dependence of the rate coefficient as shown in figure 4.

Table 1: Activation Energies Calculated by the Two Different Methods, of the Reaction Processes Observed in the Studied Alloy

Analytical Method	Activation Energies of Precipitated Phases (KJ/mol)			
	GP Zones	θ`(Al_2Cu) Phase	σ (Al_3Li) Plates	T_1(Al_2LiCu)
Kissinger	79.44	61.43	76.03	65.73
Starink	79.86	61.83	76.36	65.99
Average	*79.65*	*61.63*	*76.20*	*65.86*

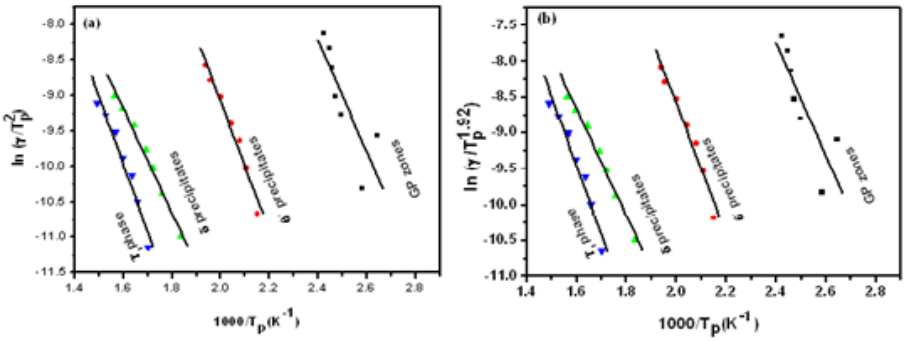

Figure 4: Relationship between (a) ln (γ/T^2_p) and ($1/T_p$) (b) ln($\gamma/T^{1.92}_p$) and ($1/T_p$) for Each Reaction Peak; (i) Clustering Process and GP-Zones Precipitation, (ii) Θ` Needle Shape Precipitation, (iii) σ Phase Precipitation and (iv) T_1 Phase for the Al-2.7%wtCu-1.8%wtLi Alloy

The activation energy associated with the clustering process and GP-zones formation was found 79.65 kJ mol^{-1}. Dutta and Allen[26] reported 33.1 kJ mol^{-1} for the GP-zones formation of 6061 alloy. Moreover, Jena et al. [27] determined an activation energy of 55.6 kJ mol^{-1} for the first process of Al–Cu–Mg alloy. Therefore, our values for the activation energy for Cu–Li-Zn vacancy clusters and GP zones process for the studied alloy are higher than the most acceptable values found in the literature. Therefore, the kinetics of the clustering process is probably contributed by coalescence of Cu-vacancy, Li-vacancy and Zn-vacancy complexes to form Li–Cu-Zn-vacancy clusters. This high activation energy indicates that the driving force of the clustering process is high which implies that, in Li-containing aluminium alloy, preferential clustering of lithium-vacancy pairs is thought to occur during solution treatment and quenching, since lithium possesses a higher vacancy binding energy than zinc or magnesium does. The preferential trapping of vacancies by lithium atoms would certainly reduce the number of free vacancies available for transport of zinc and magnesium zone forming atoms and inhibit the association of vacancies with these atoms. Decreasing the concentration of the vacancies in the matrix would make zinc and magnesium atoms less mobile, and therefore retard the clustering of zone forming atoms into zones, thus reducing the amount of zinc and magnesium zone forming atoms in zones per unit volume, and limiting the rate of aging[28]. The GP zones present consist of zinc and magnesium atoms and include some vacancies. These may be retarded as solute-rich zones. The diffusion of Zn and Mg atoms is slowed down because of preferential formation of Li-vacancy aggregates in the alloy, when Li atoms are present in the form of solution. The activation energy associated with

the precipitation of the θ` phase was found 61.63 kJ mol^{-1}. This value is close to the migration energy of Li in Al (63.7 kJ mol^{-1}), which was calculated from the activation energy of diffusion of Li in Al (135 kJ mol^{-1}) and the formation energy of vacancies in Al (71.3 kJ mol^{-1}) [29]. This value is also close to the energy of migration of Cu atoms in Al (64.7 kJ mol^{-1}), calculated as before [29].Accordingly, the mechanism of the precipitation of θ` (Al_2Cu) phase can be controlled by both migrations of Li and Cu atoms in the Al matrix. The energy associated with the δ (Al_3Li) precipitation was found 76.20 kJ mol^{-1}. This value is close to the formation energy of vacancies in Al (71.3 kJ mol^{-1}) [30]. Therefore, this precipitation process can be controlled by the migration of Cu and Li in the Al matrix, where, Li will aid in trapping excess vacancies discouraging lattice diffusion which decreases precipitate growth. However, it should be noted that the vacancy clusters that are bound to lithium atoms appear to be more stable than those formed only by rapid quenching in the alloy. Therefore, vacancies bound to lithium atoms make it difficult for diffusion or aggregate to grain boundaries, this is one of the main reasons of forming narrow precipitate-free zones in present Li-containing alloy. These results evidently indicate that Li atoms slow down the diffusion of Zn and Mg atoms and vacancies, and thus the segregation of them to grain boundaries has been restricted [28].The activation energy associated with the precipitation of the T_1 (Al_2LiCu) phase was found 65.86 kJ mol^{-1}. This value is close to the migration energy of Li in Al (63.7 kJ mol^{-1}), this value also is close to the energy of migration of Cu atoms in Al (64.7 kJ mol^{-1}), calculated as before [29]. Therefore, this precipitation process can be controlled by the migration of Cu and Li in the Al matrix.

CONCLUSIONS

Based on the combined results of DSC, HV and SEM, the following conclusions can be drawn:

- During continuous heating of Al-2.7%wtCu-1.8%wtLi (AF/C 489alloy) at a fixed heating rate of 20 K/min, six precipitation processes have taken place. Namely, Cu–Li-vacancy clustering and GP zones,initial Precipitation of θ` ($Al_2Cu$) precipitates-precipitation of δ` precipitates – precipitation of T_1 (Al_2LiCu) phase and δ (Al_3Li) phase.
- The determined activation energy of clustering process and GP ones (79.65 kJ mol^{-1}) is high indicating that its driving force is high. This causes the retardation of its precipitation (~440 K).
- According to the calculated activation energies, the kinetics of the developed strengthening precipitates can be explained as:
    - Cu–Li-vacancy clustering is controlled by coalescence of Cu-vacancy and Li-vacancy complexes to form Li–Cu-vacancy clusters.
    - θ`-precipitation is controlled mainly by migrations of Cu atoms in the Al matrix to combine with Li to form θ`(Al_2Cu).
    - The δ (Al_3Li) **and** T_1(Al_2LiCu) precipitation is controlled by the migration of Cu and Li in the Al matrix which indicates by the coexistence of them as the specimen aged at 650^{o}K for 30 min.
    - The diffusion of Zn and Mg atoms is slowed down because of preferential formation of Li-vacancy aggregates in the alloy, when Li atoms are present in the form of solution.

REFERENCES

1. I Özbek, Mater. Char., 58 (2007) 312–317
2. C. J. Williams, E. A. Starke. ActaMater., 51 (2003) 5775–99.

3. B. M. Gable, A.W. Zhu, A. A. Csontos, E.A. Starke, J. Light Met., 1 (2001) 1–14.
4. C. D. Mariora, H. Nordmark, S. J. Andersen, and R. Holmestad, J. Mater. Sci., 41(2006)471–478.
5. A. K. Shukla, W. A. Baeslack, Scr. Mater., 56 (2007) 513–516.
6. D. J. Chakrabarti and D. E. Laughlin, Prog. Mater. Sci., 49(2004) 389–410.
7. M. A. V. Huis, J. H. Chen, M. H. F. Sluiter and H. W. Zandbergen, ActaMater., 55(2007) 2183–2199.
8. B. Noble, G.E. Thomson, J. Matel. Sci., 6 (1972) 167–172.
9. P. J. Gregson and H. M. Flower, Mater. Sci. Lett., 3(1984)829-834.
10. W. Fang, L. Jinshan, H. Rui and K. Hongchao, Chin. J. of Aero., 21(2008) 565-570.
11. N. J. Kim, E.W. Lee, Acta Metall. Mater., 41 (1993) 941–948.
12. K. S. Kumar, S.A. Brown, J.R. Pickens, ActaMater., 44 (1996) 1899–1951.
13. D.Y. Li, L. Q. Chen, ActaMater., 46 (1998) 2573–2585.
14. I. J. Polmear, G. Pons, Y. Barbaux, H. Otcor, C. Sanchez, A. J. Mortan, W. E. Borbidge, S. Rogers, Mater. Sci. Technol., 15 (1999) 861–868.
15. A. Gaber, K. Matsuda, A.M. Ali, Y. Zou and S. Ikeno: Mater. Sci.Technol., 20(2004) 1627–1631.
16. A. K. Mukhopadhyay, Met. Mater. Trans., A 33 (2002) 3635–3648.
17. P.C. Bai, T.T. Zhou, P.Y. Liu, Y.G. Zhang and C.Q. Chen, Mater. Lett., 58 (2004) 3084– 3087.
18. B.C. Wei, C.Q. Chen, Z. Huang and Y.G. Zhang, Mater. Sci. Eng., A 280 (2000) 161.
19. Z.W. Huang, M.H. Loretto and J. White, Mater. Sci. Technol., 9 (1993) 967.
20. Y. J. Gu, A. Wahab, Z. Huang, Y. G. Zhang and C. Q. Chen, Mater. Sci. Eng., A 316(2001)39-45.
21. G. Itoh, Q. Cui, M. Kanno, Mater. Sci. Eng., A 211 (1996) 128–137.
22. Z. W. Du, T. T. Zhou and P. Y. Liu, Mater. Sci. Technol., 21(2005) 479-483.
23. J. C. Werenskiold, A. Deschamps and Y. Bréchet, Mater. Sci. Eng., 293A (2000) 267-274.
24. H.E. Kissinger, Anal. Chem., 29 (1957) 1702–1706.
25. M.J. Starink, Thermochim. Acta 404 (2003) 163–173.
26. Dutta and S. M. Allen, J. Mater. Sci. Lett., 10(1991)323–326.
27. A. K. Jena, A.K. Gupta and M.C. Chatuvedi, Acta Metall., 37 (1989) 885-893.
28. L.C. Doan, Y. Ohmori and K. Nakai, Mater. Trans. JIM 41 (2000) 300–305.
29. A. Gaber, M. A. Gaffar, M. S. Mostafa and E. F. Abo Zeid, J. Alloy. Compd., 429 (2007)167–175.
30. A. Gaber, A. Mossad Ali, K. Matsuda, T. Kawabata, T. Yamazaki and S. Ikeno, J. Alloy. Compd., 432 (2007) 149–155.